ACS OMEGA

Article

Cite This: ACS Omega 2019, 4, 8632−8640

http://pubs.acs.org/journal/acsodf

Evaluation of Solubility Characteristics of a Hybrid Complex of Components of Soy

Yutaka Inoue,*[,†] Mai Osada,[†] Isamu Murata,[†] Kenji Kobata,[‡] and Ikuo Kanamoto[†]

[†]Laboratory of Drug Safety Management, Faculty of Pharmacy and Pharmaceutical Sciences, Josai University, 1-1 Keyakidai, Sakado-shi, Saitama 3500295, Japan

[‡]Laboratory of Functional Food Science, Faculty of Pharmacy and Pharmaceutical Sciences, Josai University, 1-1 Keyakidai, Sakado-shi, Saitama, 3500295, Japan

ABSTRACT: The purpose of this study was to evaluate the solubilities and physicochemical properties of solid dispersions of daidzein (DDZ) and genistein (GST) (the major isoflavones in soybeans) in γ-cyclodextrin (γCD). Dispersions were prepared in distilled water using a three-dimensional ball mill (3DGMw). Phase solubility diagrams confirmed that DDZ/γCD and GST/γCD formed A_L type inclusion complexes with a molar ratio of 1:1. A new peak due to inclusion complexes was observed in the results of powder X-ray diffraction (3DGMw(DDZ/γCD = 1:1) and 3DGMw-(GST/γCD = 1:1)). Dissolution tests using distilled water found that solubilities of 3DGMw(DDZ/γCD = 1:1) and 3DGMw(GST/γCD = 1:1) were approximately 37- and 51-fold higher, respectively, than the solubilities of pure DDZ and GST. These observations are expected to expand the usefulness of cogrinding of DDZ or GST with γCD using a three-dimensional ball mill.

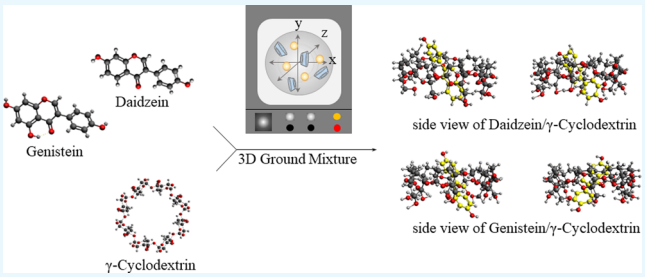

1. INTRODUCTION

Soybeans and soy products are plant-based foods extensively used worldwide. Soy products contain isoflavones, which have structures similar to the female hormone estrogen and which show estrogenic action.[1] Soy isoflavones have been reported to promote osteoplasty[2] and reduce negative symptoms of menopause.[3] Therefore, soy isoflavones are used as dietary supplements or food for specified health promoting effects. Two aglycon-type isoflavones present at relatively high concentrations in soy products are daidzein (DDZ) and genistein (GST). DDZ can reduce the risk of atherosclerotic cardiovascular disease,[4] and GST is useful for chemoprevention of prostatic cancer.[5] The improvement of dispersibility in water and the improvement of bioavailability are required for a more effective use of DDZ and GST since DDZ and GST have poor water solubility, low stability, and low bioavailability.

γ Cyclodextrin (γCD) is a complex cylindrical molecule with eight glucose molecules bonded by α1−4 linkages. Cyclodextrins have cavities in their cyclic structures and are known to form inclusion complexes that harbor other molecules,[6] thereby improving the solubility[7] and stability[8] of various pharmaceuticals. For example, formation of inclusion complexes between γCD and catechins has been reported.[9] Various methods for preparing inclusion complexes, including coprecipitation,[10] kneading,[11] freeze drying,[12] and cogrinding[13] have been reported. Cogrinding is a method of forming inclusion complexes by mechanochemical means under solvent-free conditions, changing the bonding state between two solids and the physicochemical properties of each.[14]

Cogrinding methods using a rod mill, a ball mill, a jet mill, and so on have been developed. The preparation of inclusion complexes of caffeic acid/γCD by cogrinding using a rod mill has been reported.[15] Using the ball mill, it is possible to micronize foods and tea.[16] The use of a jet mill for grinding of drugs has been reported.[17] The vibrating rod mill generates heat in the grinding process due to the mechanochemical effect. A ball mill with two-axis rotation is a type of grinder used to grind and blend materials for drug formulation. The three-dimensional (3D) ball mill has longitudinal and transverse rotational axes, enabling mixing and grinding with high uniformity. The preparation of cocrystals of ibuprofen and nicotinamide using a three-dimensional ball mill has been reported.[18] This unique grinding will operate continuously for long periods of time for powder processing. On the other hand, three-dimension ball milling is a novel grinding method that rotates in three axes. The characteristics are that it is possible to grind the drug and the material efficiently and that it does not generate heat during further grinding. In addition, there has been no report on the preparation of a ground mixture by a novel three-dimension ball mill for an inclusion complex of drug and cyclodextrin. Therefore, if it is possible to prepare inclusion complexes by a three-dimensional ball mill, this will

Received: March 16, 2019
Accepted: May 7, 2019
Published: May 16, 2019

DOI: 10.1021/acsomega.9b00733
ACS Omega 2019, 4, 8632−8640

lead to expanded application of the pharmaceutical preparation method.

Use of a three-dimensional ball mill may permit the preparation of new types of hybrid solid dispersions.

Inclusion complexes of DDZ/βCD and GST/βCD have been reported.[19] To date, the preparation of inclusion complexes of DDZ and GST using other CDs has not been reported. Therefore, we prepared solid dispersions using γCD with the aim of further improving DDZ and GST solubility. The aim of the current study was to evaluate the physicochemical properties and solubilities of DDZ/γCD and GST/γCD inclusion complexes prepared by cogrinding using a three-dimensional ball mill.

2. RESULTS AND DISCUSSION

2.1. Phase Solubility Studies. Phase solubility diagrams were obtained to determine molar ratios and stability constants of DDZ/γCD and GST/γCD inclusion complexes. The solubility of DDZ alone was 1.39 μg/mL and that of GST alone was 2.54 μg/mL after 24 h of shaking. Phase solubility diagrams indicate that the solubilities of DDZ and GST increase linearly with the addition of γCD. The inclusions formed are type A_L according to the classification of Higuchi et al. (Figure 1). A_L-type inclusions indicate a guest molecule and

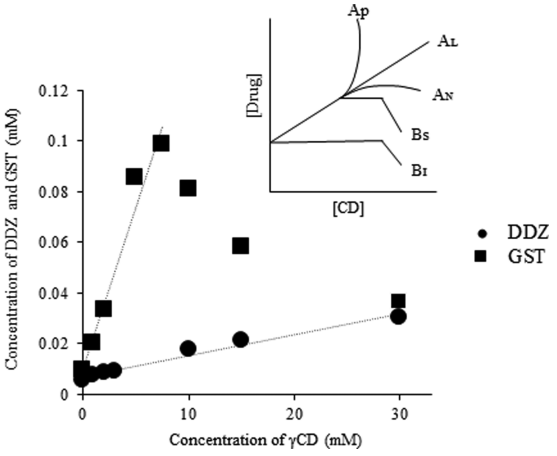

Figure 1. Phase solubility diagrams of DDZ/γCD and GST/γCD. Results were expressed as mean ± SD (n = 3).

host molecule interaction with a molar ratio of 1:1. It is suggested that DDZ and GST form 1:1 inclusion complexes with γCD in solution. Stability constant (K) was 220.85 M^{-1} for DDZ and 1378.12 M^{-1} for GST. GST is thought to form more stable inclusion complexes within γCD than DDZ since the stability constant of GST is larger than that of DDZ.

2.2. Differential Scanning Calorimetry (DSC). Phase solubility diagrams suggested that DDZ/γCD and GST/γCD complexes had 1:1 molar ratios in the aqueous solution. Solid dispersions of DDZ/γCD and GST/γCD were prepared using a three-dimensional ball mill at molar ratio of 1:1. In most reports, inclusion complex formation changes thermal behaviors, leading to disappearance of or shift in the melting points of guest molecules.[22] DSC was performed to investigate the thermal behavior of 3DGMw(DDZ/γCD) and 3DGMw-(GST/γCD) prepared using a three-dimensional ball mill. Endothermic peaks due to melting were observed at 337 °C for DDZ alone and at 301 °C for GST alone (Figure 2a,b). In PM(DDZ/γCD) and PM(GST/γCD), DDZ and GST crystals

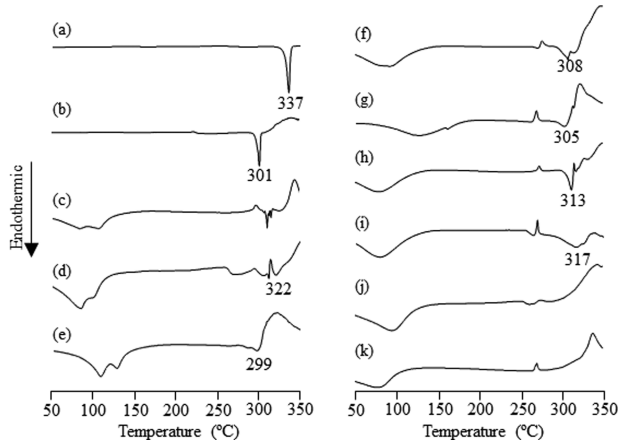

Figure 2. DSC curves of DDZ/γCD and GST/γCD systems. (a) DDZ intact, (b) GST intact, (c) γCD intact, (d) PM(DDZ/γCD = 1:1), (e) PM(GST/γCD = 1:1), (f) GM(DDZ/γCD = 1:1), (g) GM(GST/γCD = 1:1), (h) 3DGMnw(DDZ/γCD = 1:1), (i) 3DGMnw(GST/γCD = 1:1), (j) 3DGMw(DDZ/γCD = 1:1), and (k) 3DGMw(GST/γCD = 1:1).

are considered since endothermic peaks from the melting of DDZ and GST were observed at 320 and 299 °C, respectively (Figure 2d,e). Endothermic peaks from DDZ and GST were observed at 308 °C in GM(DDZ/γCD) and 305 °C in GM(GST/γCD) (Figure 2f,g). In 3DGMnw(DDZ/γCD), endothermic peaks from DDZ and GST were confirmed at 313 °C in 3DGMnw(DDZ/γCD) and 317 °C in 3DGMnw-(GST/γCD) (Figure 2h,i). Endothermic peaks from DDZ and GST disappeared in 3DGMw(DDZ/γCD) and 3DGMw-(GST/γCD) (Figure 2j,k). This data supports the conclusion that DDZ and GST are included within the cavity of γCD in 3DGMw(DDZ/γCD) and 3DGMw(GST/γCD).

2.3. Powder X-ray Diffraction (PXRD). DSC measurements suggest that 3DGMw(DDZ/γCD) and 3DGMw(GST/γCD) contain inclusion complexes. Powder X-ray diffraction was performed to investigate the crystalline states of 3DGM-(DDZ/γCD) and 3DGM(GST/γCD). Untreated DDZ, ground DDZ, and 3D ground DDZ produced characteristic diffraction peaks at 2θ of 10.2 and 24.4°. Untreated GST, ground GST, and 3D ground GST produced characteristic diffraction peaks at 2θ of 7.3 and 17.8°. γCD yielded a characteristic diffraction peak at 2θ of 9.1° (Figure 3a−g). PM(DDZ/γCD = 1:1) produced one diffraction peak corresponding to DDZ at 2θ of 24.4° and another peak at 2θ of 9.0°, corresponding to γCD (Figure 3h). PM(GST/γCD = 1:1) produced a diffraction peak at 2θ of 17.6°, corresponding to its GST component, and another peak at 2θ of 9.0°, corresponding to its γCD (Figure 3i). GM(DDZ/γCD = 1:1) produced only the diffraction peak at 2θ of 24.4°, corresponding to its DDZ. GM(GST/γCD = 1:1) produced a single diffraction peak at 2θ of 7.6°, corresponding to its GST (Figure 3j,k). Interestingly, 3DGMw(DDZ/γCD = 1:1) yielded a new peak at 2θ of 16.4° and lost the characteristic diffraction peak contributed by DDZ (Figure 3n). 3DGMw-(GST/γCD = 1:1) also yielded a new peak at 2θ of 16.5° and lost the characteristic diffraction peak contributed by GST (Figure 3o). These results suggested that DDZ/γCD and GST/γCD formed novel complexes upon cogrinding with a three-dimensional ball mill. It is generally accepted that inclusion complexes are formed by mechanochemical effects of grinding.[23] GM(DDZ/γCD) and GM(GST/γCD) that

DOI: 10.1021/acsomega.9b00733
ACS Omega 2019, 4, 8632−8640

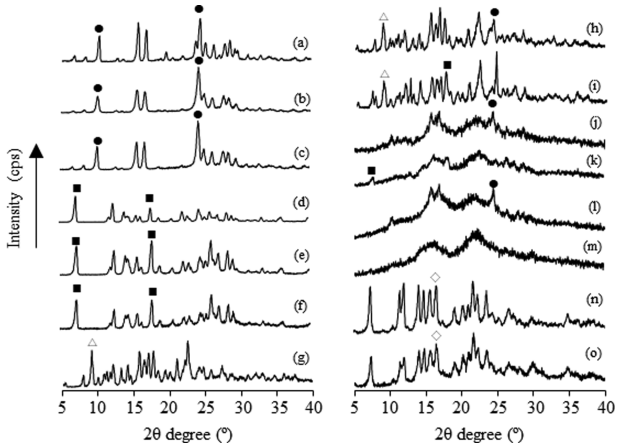

Figure 3. PXRD patterns of DDZ/γCD and GST/γCD. (a) DDZ intact, (b) DDZ ground, (c) DDZ 3D ground, (d) GST intact, (e) GST ground, (f) GST 3D ground, (g) γCD intact, (h) PM(DDZ/γCD = 1:1), (i) PM(GST/γCD = 1:1), (j) GM(DDZ/γCD = 1:1), (k) GM(GST/γCD = 1:1), (l) 3DGMnw(DDZ/γCD = 1:1), (m) 3DGMnw(GST/γCD = 1:1), (n) 3DGMw(DDZ/γCD = 1:1), and (o) 3DGMw(GST/γCD = 1:1). ●, DDZ original; ■, GST original; Δ, γCD original; ◇, new peak.

were coground using a rod mill did not produce any new peaks. This method apparently lowered inclusion efficiency as grinding produced heat. When dry DDZ and GST were coground with γCD using a three-dimensional ball mill, DDZ and GST did not form inclusion complexes with γCD since they were not adequately dispersed and mixed. However, when DDZ and GST were coground with γCD in distilled water using a three-dimensional ball mill, inclusion complexes formed, as the distilled water promoted entry of DDZ and GST into the cavity of γCD.

2.4. Near-Infrared Absorption Spectroscopy (NIR).

The results of DSC and PXRD suggested the possibility that inclusion complexes are forming in 3DGMw. Therefore, NIR measurements were performed to investigate the molecular structure of the complexes in the solid state. DDZ intact produced a peak at 4836 $cm^{-1,}$ corresponding to the hydroxy group derived from its aromatic ring, and a peak at 4456 cm^{-1}, to corresponding with the alkyl group (Figure 4A). The peak produced by the hydroxy group attached to its aromatic ring shifts to 4824 cm^{-1}, and the peak produced by the alkyl group shifts to 4396 cm^{-1} in GM(DDZ/γCD). The peak produced by the hydroxy group attached to the aromatic ring of DDZ shifts to 4792 cm^{-1}, and the peak produced by the alkyl group shifts to 4412 cm^{-1} in 3DGMw(DDZ/γCD). Unground γCD alone produces a peak at 7024 cm^{-1}, corresponding to its hydroxy group. The peak produced by the hydroxy group derived from γCD shifts to 7008 cm^{-1} and broadens in GM(DDZ/γCD). This same peak shifts to 7000 cm^{-1} and broadens in 3DGMw(DDZ/γCD). 3DGMw(DDZ/γCD) was confirmed to broaden this peak more than GM(DDZ/γCD). Finally, unground GST alone produced a peak at 4848 cm^{-1}, corresponding to the hydroxy group attached to its aromatic ring, and a peak at 4424 cm^{-1}, corresponding to its alkyl group (Figure 4B). The peak produced by the hydroxy group on the aromatic ring of GST shifts to 4844 cm^{-1}, and the peak produced by the alkyl group shifts to 4400 cm^{-1} in GM(GST/γCD). The peak produced by the hydroxy group on the aromatic ring of GST shifts to 4792 cm^{-1}, and the peak produced by the alkyl group shifts to 4408 cm^{-1} in 3DGMw(GST/γCD). The peak produced by the hydroxy group of γCD shifts to 7012 cm^{-1} and broadens in

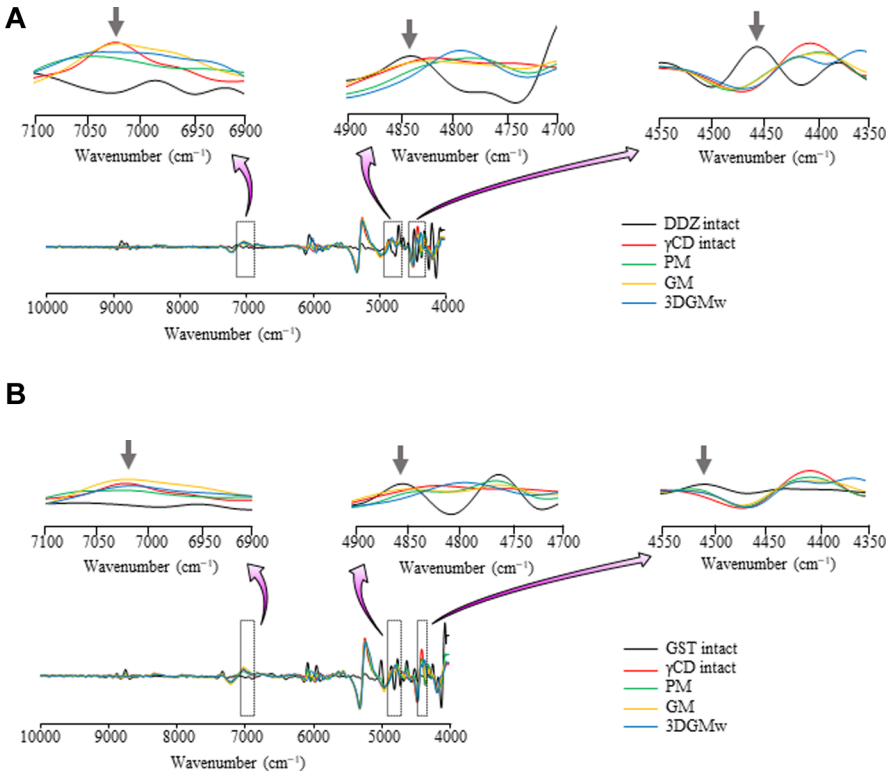

Figure 4. (A) NIR absorption spectra of DDZ/γCD systems. (B) NIR absorption spectra of GST/γCD systems.

DOI: 10.1021/acsomega.9b00733
ACS Omega 2019, 4, 8632−8640

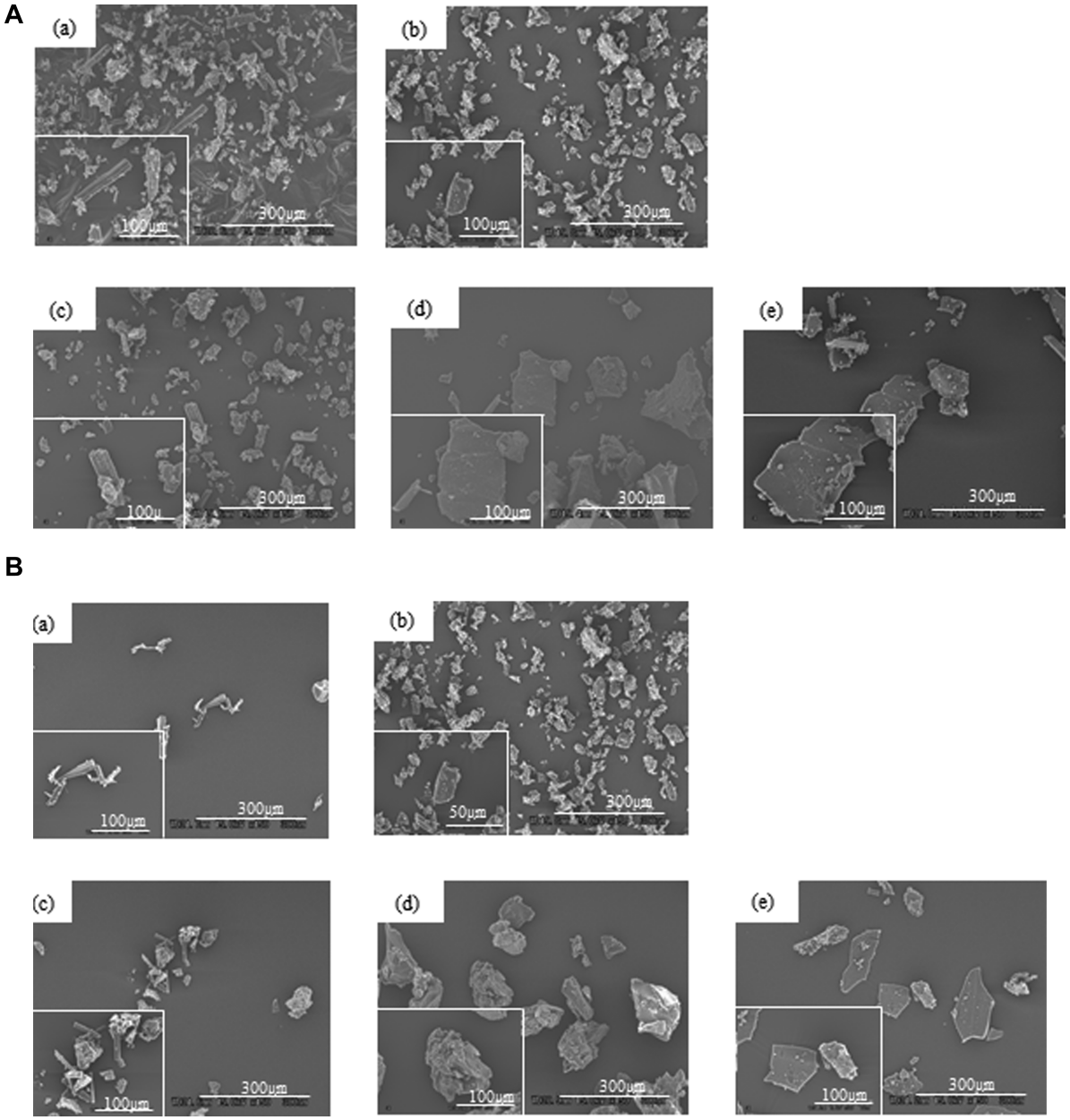

Figure 5. (A) SEM micrographs of DDZ/γCD systems: (a) DDZ intact, (b) γCD intact, (c) PM(DDZ/γCD = 1:1), (d) GM(DDZ/γCD = 1:1), and (e) 3DGMw(DDZ/γCD = 1:1). (B) SEM micrographs of GST/γCD systems: (a) GST intact, (b) γCD intact, (c) PM(GST/γCD = 1:1), (d) GM(GST/γCD = 1:1), and (e) 3DGMw(GST/γCD = 1:1).

3DGM(GST/γCD) compared to that of unground γCD alone. This shift and broadening suggest that 3DGMw(DDZ/γCD) and 3DGMw(GST/γCD) have intermolecular hydrogen bonding in the solid state between groups in the cavity of γCD and between groups on DDZ and GST.

2.5. Scanning Electron Microscopy (SEM). The results of DSC and PXRD for 3DGMw(DDZ/γCD) and 3DGMw-(GST/γCD) suggest the formation of an insertion complex. In addition, PXRD confirmed that the crystal state changes upon 3D cogrinding. Therefore, SEM was performed to observe the shape and surface of the crystal formed. DDZ was smooth and had a columnar shape with a length of around 100 μm (Figure 5A (a)). GST was smooth and had an acicular shape with a length of around 50 μm (Figure 5B(a)). γCD was angular, smooth, and its particle diameter was around 20 μm (Figure 5A(b)). In PM(DDZ/γCD) and PM(GST/γCD), we observed crystals similar to those of pure DDZ, GST, and γCD (Figure 5A(c),B(c)). GM(DDZ/γCD) and GM(GST/γCD) crystals were 100 μm in diameter, rough, and looked like aggregates of small fragments (Figure 5A(d),B(d)). 3DGMw-(DDZ/γCD) and 3DGMw(GST/γCD) crystals were 100 μm in diameter, rough, and angular (Figure 5A(e),B(e)). Generally, inclusions formed by γCD have been described as cubic.[24] Our studies confirmed 3DGMw(DDZ/γCD) and 3DGMw(GST/γCD) crystals to have a cubic shape. It is thought that DDZ and GST are more likely to form inclusion complexes with γCD in the solid state.

2.6. Measurement of ^{1}H−^{1}H Nuclear Overhauser Effect Spectroscopy (NOESY) NMR Spectra. ^{1}H−^{1}H NOESY NMR was performed to examine intermolecular interactions between 3DGMw(DDZ/γCD) and 3DGMw-(GST/γCD) in solution. ^{1}H−^{1}H NOESY NMR was used to

DOI: 10.1021/acsomega.9b00733
ACS Omega 2019, 4, 8632−8640

infer the relative position of the inclusion complex since it can confirm interactions between the guest molecule and the CD cavity. 3DGMw(DDZ/γCD) produced cross peaks between the H-3 proton (3.75 ppm) in the γCD cavity and the H-a proton (7.7 ppm), the H-e, h proton (7.05 ppm), and the H-d proton (6.3 ppm) of the DDZ (Figure 6A). In 3DGMw(GST/γCD), cross peaks were confirmed between the H-3 proton (3.74 ppm) in the γCD cavity and the H-f, g proton (6.7 ppm) and the H-c proton (6.0 ppm) of the GST (Figure 6B). It is generally known that the H-3 proton is at the wide edge of the CD ring and the H-6 proton is at the narrow edge of the CD ring. Thus, this data suggests the formation of two types of inclusion complexes in which DDZ molecules are enclosed with their phenyl group or their resorcinol moiety facing the narrower edge of the γCD ring (Scheme 1A). Similarly, the data suggests two inclusion types in which GST molecules are enclosed with their phenyl group or their resorcinol moiety facing the narrow edge of the γCD ring (Scheme 1B). It has previously been reported that the DDZ/βCD solid dispersion has two types of inclusion modes.[25] These results suggest that DDZ/γCD and GST/γCD have similar inclusion modes.

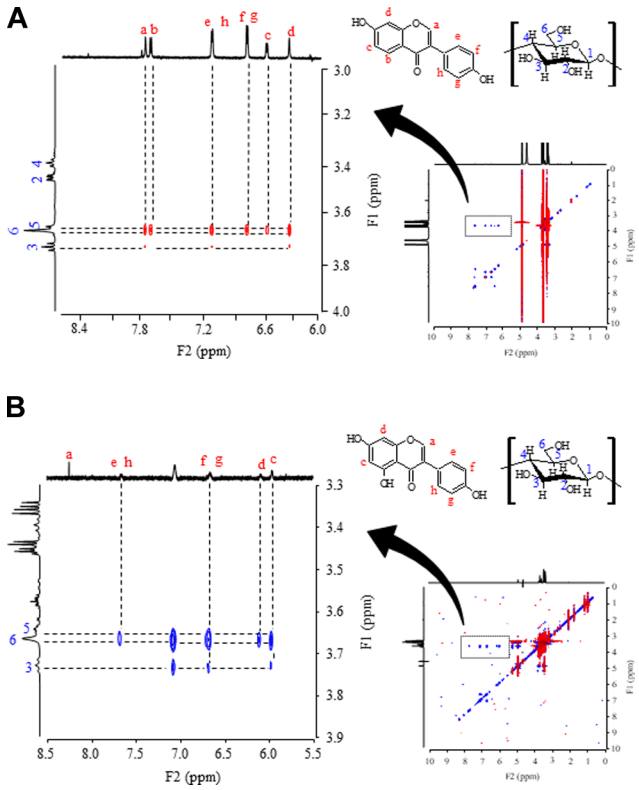

Figure 6. A) $^{1}H-^{1}H$ NOESY NMR spectrum of DDZ/γCD systems. (B) $^{1}H-^{1}H$ NOESY NMR spectrum of GST/γCD systems.

2.7. Dissolution Profile (Distilled Water). The results of DSC, PXRD, and NIR suggested the possibility that inclusion complexes formed in the solid state in 3DGMw(DDZ/γCD) and 3DGMw(GST/γCD). Therefore, dissolution tests were performed to investigate whether dissolution behavior of DDZ and GST changed due to inclusion complex formation. The concentration of unground DDZ alone after 5 min was 0.18 μg/mL. The concentration was 0.19 μg/mL for ground DDZ and 1.49 μg/mL for 3D ground DDZ (Figure 7A). The concentration of unground GST alone after 5 min was 0.19 μg/mL. The concentration was 0.43 μg/mL for ground GST and 0.37 μg/mL for 3D ground GST (Figure 7B). Concentrations of DDZ were 0.17 μg/mL in PM(DDZ/γCD), 5.77 μg/mL in GM(DDZ/γCD), and 6.08 μg/mL in 3DGMnw(DDZ/γCD) after 5 min. Both ground mixtures with γCD yielded higher dissolution than DDZ alone. Concentrations of GST were 0.25 μg/mL in PM(GST/γCD), 5.48 μg/mL in GM(GST/γCD), and 3.66 μg/mL in 3DGMnw-(GST/γCD) after 5 min. Concentrations of DDZ and GST in 3DGMw(DDZ/γCD) and 3DGMw(GST/γCD) after 5 min were 6.78 and 8.60 μg/mL. The solubility was notably improved by 3D grinding compared to that of unground DDZ or GST alone. The results of the phase solubility diagrams indicated that the solubility of GST/γCD was higher than that of DDZ/γCD because the solubility of GST alone was higher than that of DDZ alone. Improvements in

Scheme 1. Proposed Structural Images of DDZ/γCD and GST/γCD Complexes[a]

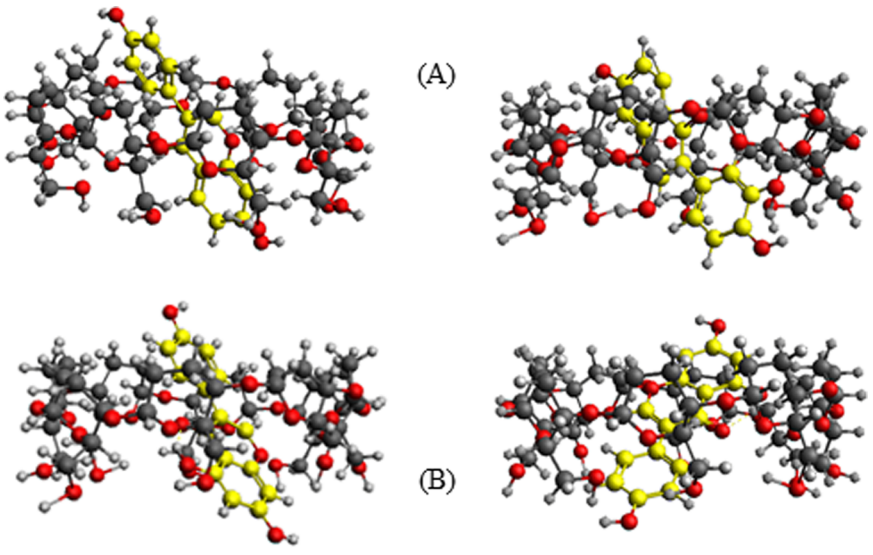

[a](A) Side view of 3DGMw(DDZ/γCD) and (B) side view of 3DGMw(GST/γCD).

DOI: 10.1021/acsomega.9b00733
ACS Omega 2019, 4, 8632−8640

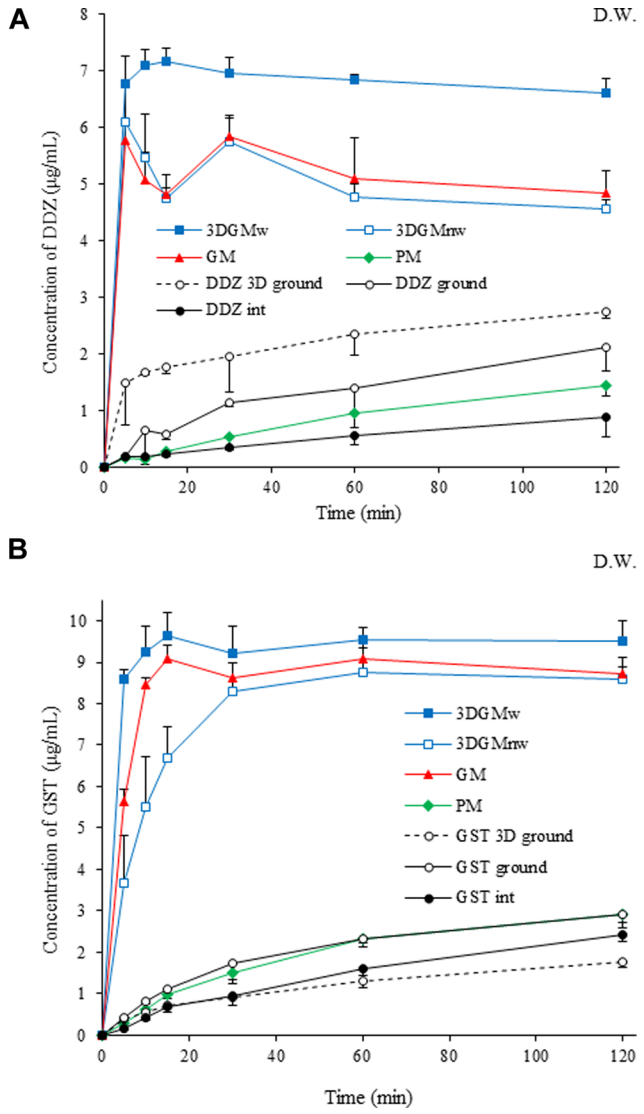

Figure 7. (A) Dissolution profiles of DDZ/γCD systems. Results were expressed as mean ± SD (n = 3). (B) Dissolution profiles of GST/γCD systems. Results were expressed as mean ± SD (n = 3).

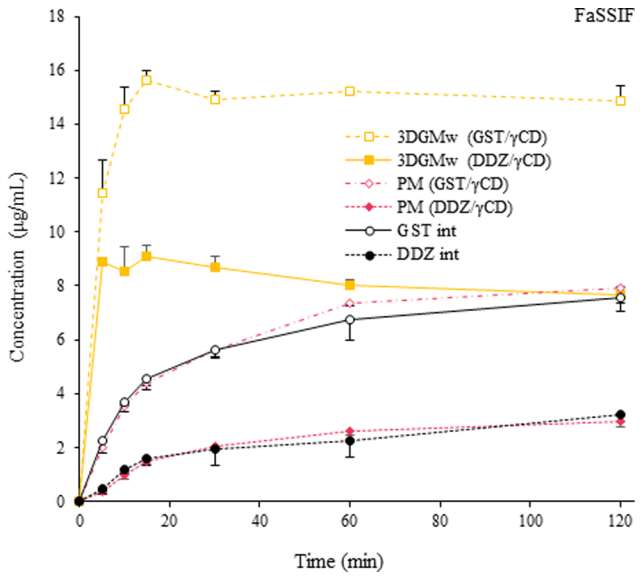

Figure 8. Dissolution profiles of DDZ/γCD and GST/γCD systems using FaSSIF. Results were expressed as mean ± SD (n = 3).

solubilities of DDZ in 3DGMw(DDZ/γCD) and GST in 3DGMw(GST/γCD) are attributable to inclusion complex formation. The relatively low solubilities of GM(DDZ/γCD), GM (GST/γCD), 3DGMnw(DDZ/γCD), and 3DGMnw-(GST/γCD) compared to those of 3DGMw(DDZ/γCD) and 3DGMw(GST/γCD) can be explained by failure to form inclusion complexes. This conclusion is supported by our observation of the characteristic diffraction peaks of DDZ and GST alone in the above mixtures in PXRD. Our results indicate that cogrinding in distilled water using a three-dimensional ball mill can improve the solubilities of DDZ and GST.

2.8. Dissolution Profile (Fasted State Simulated Intestinal Fluid—FaSSIF). Dissolution tests were performed to confirm the solubilities of DDZ alone, PM(DDZ/γCD), 3DGMw(DDZ/γCD), GST intact, PM(GST/γCD), and 3DGMw(GST/γCD) in the intestinal fluid. The concentration of DDZ alone was 0.48 μg/mL. The concentration of PM(DDZ/γCD) was 0.36 μg/mL after 5 min (Figure 8). The concentration of GST alone was 2.24 μg/mL, whereas the concentration of PM(GST/γCD) was 1.97 μg/mL after 5 min. The concentrations of DDZ and GST in 3DGMw(DDZ/γCD) and 3DGMw(GST/γCD) after 5 min were 8.91 and 11.43 μg/mL. Improved dissolution of 3DGMw(DDZ/γCD) and 3DGMw(GST/γCD) in the intestinal fluid was confirmed. CoQ10/γCD inclusion complexes can facilitate CoQ10 incorporation into NaTC when CoQ10/γCD inclusion complexes are dissolved in NaTC solution. CoQ10 can be released in solution from CoQ10/γCD inclusion complexes, and the released CoQ10 forms micelles with NaTC.[26] It has been speculated that DDZ/γCD and GST/γCD inclusion complexes dissolved in FaSSIF solution allow DDZ and GST to be incorporated into NaTC since NaTC is contained in FaSSIF solution. Inclusion complexes prepared for DDZ/βCD with coprecipitation using an organic solvent have been reported.[19] We found that the DDZ or GST/βCD inclusion complex was prepared using a three-dimension ball mill as a new convenient grinding method. We have already reported that the stability constant of the caffeic acid/βCD inclusion complex was higher than that of the caffeic acid/αCD or γCD inclusion complex.[15] If it is possible to prepare for DDZ or GST/αCD orβCD using the three-dimension ball mill method, this would confirm comparing stability constants and differences of solubility with αCB and βCD. Since the solubility of the DDZ or GST/γCD complex is improved under FaSSIF conditions, when an animal experiment was carried out to improve the bioavailability of DDZ and GST might be expected.

In the result of this study, we made a new inclusion complex of DDZ or GST/γCD. Thus, we need to study the difference in the DDZ or GST/CD complex formation between those involving αCD rings and those involving βCD rings.

2.9. DPPH Radical Scavenging. Results of the DPPH radical scavenging test indicated that ascorbic acid inhibited DPPH radical scavenging, with a 50% inhibitory concentration (IC_{50}) of 4.79 μg/mL; the IC_{50} value for intact DDZ was 352.89 μg/mL (Figure 9). In addition, the IC_{50} value for 3DGMw(DDZ/γCD) was 265.46 μg/mL, which was significantly lower than the IC_{50} value for intact DDZ. The IC_{50} value for 3DGMw (GST/γCD) was 165.0 μg/mL, which was

DOI: 10.1021/acsomega.9b00733
ACS Omega 2019, 4, 8632−8640

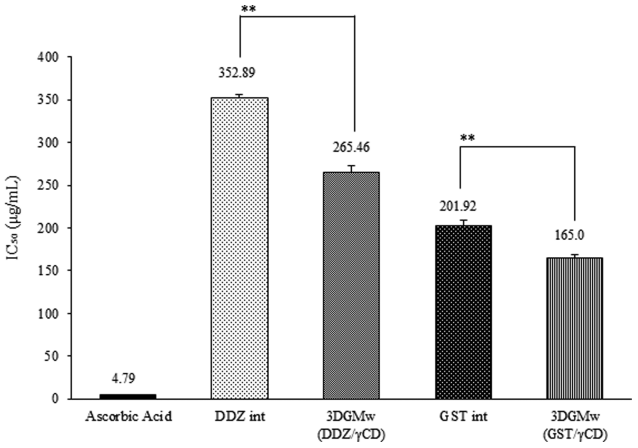

Figure 9. IC_{50} of DDZ/γCD and GST/γCD systems in a DPPH radical scavenging test. Results are expressed as mean ± SD (n = 3). **p < 0.01 vs DDZ or GST (Tukey's test).

significantly lower than the IC_{50} value for intact GST (201.92 μg/mL).

Electron density increased in the presence of DDZ or GST molecules in the γCD molecule. As a result, the DDZ and GST molecules are more likely to release protons and, subsequently, scavenge DPPH radicals.[21] It is known that the stability constant of an aqueous solution affects its antioxidant capacity.[27] GST/γCD tended to have a higher antioxidant capacity since the results of the phase solubility study indicated that GST/γCD had a higher stability constant than DDZ/γCD.

3. CONCLUSIONS

In this study, DDZ/γCD and GST/γCD inclusion complexes were prepared by cogrinding using a three-dimensional ball mill. Structural data on 3DGMw(DDZ/γCD) and 3DGMw-(GST/γCD) inclusion complexes confirmed the formation of two types of complexes in which either the phenyl groups or the resorcinol moieties of DDZ and GST were encapsulated. Improved solubilities of 3DGMw(DDZ/γCD) and 3DGMw-(GST/γCD) due to inclusion complex formation were confirmed. Improved solubilities of DDZ/γCD and GST/γCD complexes in FaSSIF indicated that the impact of inclusion complex formation will be physiologically relevant in vivo. These results are expected to expand the use of three-dimensional ball mill grinding beyond its application to mixing DDZ and GST with γCD. The three-dimensional ball mill will play a part in a novel composite preparation method in the pharmaceutical field.

4. MATERIALS AND METHODS

4.1. Materials. Daidzein (DDZ) (Figure 10a) was purchased from Kokusan Chemical Co., Ltd. Genistein (GST) (Figure 10b) was purchased from Ark Pharm, Inc. γCD (Figure 10c) was a generous gift from CycloChem Bio Co., Ltd. (Tokyo, Japan) and was stored at 40 °C and 82% relative humidity for 7 days. All other chemicals were of analytical grade and were purchased from FUJIFILM Wako Pure Chemical Corporation, Tokyo.

4.2. Preparation of the Physical Mixture (PM), Ground Mixture (GM), and 3D Ground Mixture (3DGM). PM(DDZ/γCD) and PM(GST/γCD) were made by mixing DDZ or GST with γCD in 1:1 molar ratios using a vortex mixer for 1 min. GM(DDZ/γCD) and GM(GST/γCD) were made by grinding PM(DDZ/γCD) and PM(GST/γCD) (1 g of the total of each) for 60 min using a vibration rod mill (TI-500ET, CMT Co. Ltd., Japan). 3DGM(DDZ/γCD) and 3DGM(GST/γCD) were made by grinding PM(DDZ/γCD) or PM(GST/γCD) (500 mg total of each) using a three-dimension ball mill with a 200 g ball of Φ5 mm for 60 min plus (3DGMw) or minus (3DGMnw) 500 μL of distilled water.

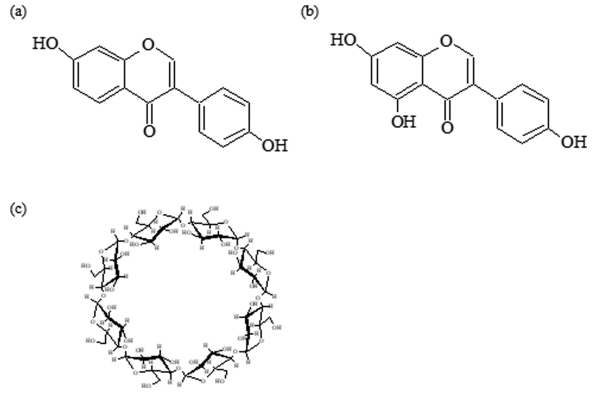

Figure 10. Chemical structures: (a) daidzein (DDZ), (b) genistein (GST), and (c) γ-cyclodextrin (γCD).

4.3. Methods. *4.3.1. Phase Solubility Study.* Solubility studies were conducted according to the method of Higuchi and Connors.[20] Ten milliliter of distilled water was added to 20 mg of each of DDZ and GST, yielding supersaturated solutions of each. Concentrations of γCD ranging from 0 to 30 mM were added, and suspensions were obtained by shaking at 100 rpm and 25 ± 0.5 °C for 24 h using a constant-temperature shaking culture machine (BR 42 FL, TAITEC Co., Ltd.). Solutions at equilibrium were filtered through 0.2 μm membrane filters (hydrophilic poly(tetrafluoroethylene) type, DISMIC), and solution concentrations were quantitated. Apparent stability constants (K_s) of DDZ/γCD and GST/γCD inclusion complexes were calculated from slopes of phase solubility diagrams, and solubilities of DDZ and GST in the absence of γCD (S_0) were determined using eq 1

$$K_s = \frac{\text{slope}}{S_0(1 - \text{slope})} \quad (1)$$

4.3.2. Quantitation of DDZ and GST by High-Performance Liquid Chromatography (HPLC). Solubility was quantified by high-performance liquid chromatography (HPLC: LC-20ADvp, SHIMADZU CORPORATION) using an Inertsil ODS-3 (4.6 × 150 mm^2, Φ5 μm) column and a detection wavelength of 250 nm. The sample injection volume was 30 μL, and the column temperature was 40 °C. The mobile phase for DDZ consisted of acetonitrile/distilled water/acetic acid (25:67.5:7.5). The DDZ retention time was adjusted to 6 min. The mobile phase for GST consisted of acetonitrile/methanol/distilled water/acetic acid (30:15:55:0.1), and the GST retention time was adjusted to 6 min.

4.3.3. Differential Scanning Calorimetry (DSC). The thermal behavior of samples was recorded using a differential scanning calorimeter (Thermo plus EVO, Rigaku Co, Tokyo). All samples were weighed (2 mg) and heated and scanned at a rate of 10.0 °C/min under a nitrogen flow (60 mL/min). Aluminum crimp pans were used for all samples.

DOI: 10.1021/acsomega.9b00733
ACS Omega 2019, 4, 8632−8640

4.3.4. Powder X-ray Diffraction (PXRD). A MiniFlex II powder X-ray diffractometer (Rigaku Corporation, Tokyo) was used to perform PXRD. The diffraction intensity was measured using a NaI scintillation counter. PXRD was performed using Cu Kα radiation (30 kV, 15 mA), a scan rate of 4°/min, and a scan range of 2θ = 5−40°. Powder samples were held between glass plates to yield a flat sample plane when measurements were performed.

4.3.5. Near-Infrared (NIR) Absorption Spectroscopy. Fourier transform near-infrared absorption spectroscopy (Buchi NIR Flex N-500: Nihon Buchi) was used to perform NIR. Measurement conditions were as follows: wave number was 10 000−4000 cm^{-1}, scan time was 8 s, and scan temperature was 40 °C. Each sample was placed into a sample cup, and measurements were performed at intervals of 1 nm on the optical path.

4.3.6. Scanning Electron Microscopy (SEM). An S3000 N scanning electron microscope (Hitachi High-Technologies Corporation) was used to perform SEM. Gold was deposited on each sample for 70 s, and microscopy was performed at an accelerating voltage of 10 kV.

4.3.7. Measurement of $^1H-^1H$ Nuclear Overhauser Effect Spectroscopy (NOESY) NMR Spectra. A 700 MHz NMR system (Agilent Technologies) was used to perform NMR. The solvent was D_2O. The resonance frequency was 699.6 MHz, pulse width was 45°, relaxation delay was 1.500 s, and temperature was 25 °C with 256 increments.

4.3.8. Dissolution Profile. Dissolution tests were performed using the paddle method of the JP17 revised dissolution test on an NTR-593 dissolution apparatus (Toyama Sangyo Co. Ltd., Japan). Nine hundred milliliter of distilled water (37 ± 0.5 °C) and 300 mL of fasted state simulated intestinal fluid (FaSSIF) (37 ± 0.5 °C) were stirred at 50 rpm. Ten milligrams of each of DDZ and GST were accurately weighed and added to the paddle apparatus. Ten milliliter of each dissolved sample was collected at 5, 10, 15, 30, 60, and 120 min and filtered through 0.2 μm membrane filters. To keep the total solution volume constant, an equal volume of solution held at the same temperature was added to the paddle apparatus after each sample was collected. Quantitation was performed by the same method as was used in phase solubility studies.

4.3.9. Preparation of Fasted State Simulated Intestinal Fluid (FaSSIF). To prepare 500 mL of FaSSIF, 500 mL of the stock solution was used to dissolve sodium dihydrogen phosphate to a final concentration of 31.526 mM and sodium chloride to a final concentration of 116.6 mM. The pH was adjusted to 6.5 with sodium hydroxide. Sodium taurocholate (NaTC) was dissolved to a final concentration of 3 mM using 125 mL of stock solution. Biochemistry-grade lecithin (0.75 mM) was dissolved in 3 mL of dichloromethane in a recovery flask. The NaTC solution (125 mL) was added to the lecithin solution while applying ultrasound. The resulting solution was depressurized with a rotary evaporator (Rotavapor R-215, Nihon Buchi) at 40 °C for 15 min at 100 mbar. Once the white turbid solution became clear, if the odor of dichloromethane was detected, vacuum was applied for 5 min at 50 mbar. The depressurized solution was put into a 500 mL volumetric flask. The recovery flask was washed with the remaining 325 mL of stock solution, which was then added to the volumetric flask. Subsequent mixtures were prepared in the same 500 mL volumetric flask using a portion of the solution to wash the other recovery flasks and containers used to prepare the FaSSIF solution.

4.3.10. DPPH Radical Scavenging Test. A DPPH radical scavenging test was performed using a Spectra Max 190 microplate reader (Molecular Devices Japan Co., Ltd., Tokyo, Japan). Each sample was dissolved in equal volumes of methanol and phosphate buffer, pH 6.8 (second fluid in the revised JP17 dissolution test [second fluid]), and then filtered through 0.2 μm membrane filters. A DPPH/methanol solution (500 μm) was mixed in a microplate at a volume ratio of 4:1. The mixture was then incubated at 37 °C for 50 min while being shielded from light, and the absorbance (As) of DPPH was measured at a wavelength of 517 nm. A mixture of methanol/second fluid/DPPH methanol (2:2:1) with a rate of radical removal of 0% (A_0) and a mixture of methanol/second fluid (3:2) with a rate of radical removal of 100% (Blank, Bl) were prepared. The radical scavenging rate was calculated using eq 2[21]

$$\text{radical scavenging rate} = [1 - (\text{As} - \text{Bl})/(A_0 - \text{Bl})] \times 100 \quad (2)$$

4.3.11. Statistical Analysis. Data are expressed as the mean ± standard deviation (SD). Groups were compared using one-way analysis of variance followed by Tukey's test for multiple comparison. $p < 0.01$ was considered statistically significant.

AUTHOR INFORMATION

Corresponding Author

*E-mail: yinoue@josai.ac.jp. Tel/Fax: +81-49-271-7317.

Funding

This research was supported by Josai University.

Notes

The authors declare no competing financial interest.

ACKNOWLEDGMENTS

The authors wish to thank Dr. T. Tarumi of Japan Buchi Co., Ltd. for his helpful advice regarding NIR absorption measurements. We also acknowledge S. Shimizu and Titapha Ruangrajitpakor for their assistance in conducting these experiments. We would like to thank Dr. F. Nagao of Japan Nagao System Inc. for providing a three-dimensional ball mill.

ABBREVIATIONS

DDZ, daidzein; GST, genistein; γCD, γcyclodextrin; PM, physical mixture; GM, ground mixture; 3DGM, 3D ground mixture; DSC, differential scanning calorimeter; PXRD, powder X-ray diffraction; NIR, near-infrared absorption spectrometry; SEM, scanning electron microscopy; NMR, nuclear magnetic resonance; FaSSIF, fasted state simulated intestinal fluid; second fluid, second fluid in the revised JP17 dissolution test

REFERENCES

(1) Wood, C. E.; Register, T. C.; Franke, A. A.; Anthony, M. S.; Cline, J. M. Dietary Soy Isoflavone Inhibit Estrogen Effects in the Postmenopausal Breast. *Cancer Res.* **2006**, *66*, 1241−1249.

(2) Arjmandi, B. H.; Smith, B. J. Soy isoflavones' osteoprotective role in postmenopausal women: mechanism of action. *J. Nutr. Biochem.* **2002**, *13*, 130−137.

(3) Messina, M.; Hughes, C. Efficacy of soyfoods and soybean isoflavone supplements for alleviating menopausal symptoms is positively related to initial hot flush frequency. *J. Med. Food* **2003**, *6*, 1−11.

DOI: 10.1021/acsomega.9b00733
ACS Omega 2019, 4, 8632−8640

(4) Pan, W.; Ikeda, K.; Takebe, M.; Yamori, Y. Daidzein and Glycitein Inhibit Growth and DNA Synthesis of Aortic Smooth Muscle Cells from Stroke-Prone Spontaneously Hypertensive Rats. *J. Nutr.* **2001**, *131*, 1154−1158.
(5) Kurahashi, N.; Iwasaki, M.; Sasazuki, S.; Otani, T.; Inoue, M.; Tsugane, S. Soy product and isoflavone consumption in relation to prostate cancer in Japanese men. *Cancer Epidemiol., Biomarkers Prev.* **2007**, *16*, 538−545.
(6) Brewster, M. E.; Loftsson, T. Cyclodextrins as pharmaceutical solubilizers. *Adv. Drug Delivery Rev.* **2007**, *59*, 645−666.
(7) Kakran, M.; Sahoo, N. G.; Li, L.; Judeh, Z. Dissolution Enhancement of artemisinin with β-cyclodextrin. *Chem. Pharm. Bull.* **2011**, *59*, 646−652.
(8) Antony Muthu, P. A.; Subramanian, V. K.; Rajendiran, N. Excimer formation in inclusion complexes of β-cyclodextrin with salbutamol, sotalol and atenolol: Spectral and molecular modeling studies. *Spectrochim. Acta, Part A* **2012**, *96*, 95−107.
(9) Ishizu, T.; Tsutsumi, H.; Yamamoto, H.; Harano, K. NMR spectroscopic characterization of inclusion complexes comprising cyclodextrins and gallated catechins in aqueous solution: cavity size dependency. *Magn. Reson. Chem.* **2009**, *47*, 283−287.
(10) Ghosh, A.; Biswas, S.; Ghosh, T. Preparation and Evaluation of Silymarin β-cyclodextrin Molecular Inclusion Complexes. *J. Young Pharm.* **2011**, *3*, 205−210.
(11) Sambasevam, K. P.; Mohamad, S.; Sarih, N. M.; Ismail, N. A. Synthesis and Characterization of the Inclusion Complex of β-cyclodextrin and Azomethine. *Int. J. Mol. Sci.* **2013**, *14*, 3671−3682.
(12) Talegaonkar, S.; Khan, A. Y.; Khar, R. K.; Ahmad, F. J.; Khan, Z. I. Development and Characterization of Paracetamol Complexes with Hydroxypropyl-β-Cyclodextrin. *Iran. J. Pharm. Res.* **2007**, *6*, 95−99.
(13) Shiozawa, R.; Inoue, Y.; Murata, I.; Kanamoto, I. Effect of antioxidant activity of caffeic acid with cyclodextrins using ground mixture method. *Asian J. Pharm. Sci.* **2018**, *13*, 24−33.
(14) Cugovčan, M.; Jablan, J.; Lovrić, J.; Cinčić, D.; Galić, N.; Jug, M. Biopharmaceutical characterization of praziquantel cocrystals and cyclodextrin complexes prepared by grinding. *J. Pharm. Biomed. Anal.* **2017**, *137*, 42−53.
(15) Inoue, Y.; Suzuki, K.; Ezawa, T.; Murata, I.; Yokota, M.; Tokudome, Y.; Kanamoto, I. Examination of the physicochemical properties of caffeic acid complexed with γ-cyclodextrin. *J. Inclusion Phenom. Macrocyclic Chem.* **2015**, *83*, 289−298.
(16) Wu, D.; Wu, C.; Chen, H.; Wang, Z.; Yu, C.; Du, M. Effect of Ball Mill Treatment on the Physicochemical Properties and Digestibility of Protein Extracts Generated from Scallops (*Chlamys farreri*). *Int. J. Mol. Sci.* **2018**, *19*, No. 531.
(17) Loh, Z. H.; Samanta, A. K.; Sia Heng, P. W. Overview of milling techniques for improving the solubility of poorly water-soluble drugs. *Asian J. Pharm. Sci.* **2015**, *10*, 255−274.
(18) *The 32nd Annual Meeting The Academy of Pharmaceutical Science and Technology*; Academy of Pharmaceutical Science and Technology, Japan (APSTJ): Japan, Omiya, 2017. http://nagaosystem.co.jp/pdf/170510.pdf.
(19) Lee, S. H.; Kim, Y. H.; Yu, H. J.; Cho, N. S.; Kim, T. H.; Kim, D. C.; Chung, C. B.; Hwang, Y. I.; Kim, K. H. Enhanced bioavailability of soy isoflavones by complexation with beta-cyclodextrin in rats. *Biosci., Biotechnol., Biochem.* **2007**, *71*, 2927−2933.
(20) Higuchi, T.; Connors, K. A. Phase-solubility techniques. *Adv. Anal. Chem. Instrum.* **1961**, *4*, 117−212.
(21) Chao, J.; Hongfang, W.; Wei, Z.; Min, Z.; Liwei, Z. Investigation of the inclusion behavior of chlorogenic acid with hydroxypropyl-β-cyclodextrin. *Biol. Macromol.* **2012**, *50*, 277−282.
(22) Ficarra, R.; Ficarra, P.; Di Bella, M. R.; Raneri, D.; Tommasini, S.; Calabrò, M. L.; Gamberini, M. C.; Rustichelli, C. Study of β-blockers/β-cyclodextrins inclusion complex by NMR, DSC, X-ray, and SEM investigation. *J. Pharm. Biomed. Anal.* **2000**, *23*, 33−40.
(23) Ramos, A. I.; Braga, T. M.; Silva, P.; Fernandes, J. A.; Ribeiro-Claro, P.; de Fátima Silva Lopes, M.; Almeida Paz, F. A.; Braga, S. S. Chloramphenicol-cyclodextrin inclusion compounds: co-dissolution and mechanochemical preparations and antibacterial action. *CrystEngComm* **2013**, *15*, 2822−2834.
(24) Prabu, S.; Sivakumar, K.; Swaminathan, M.; Rajamohan, R. Preparation and characterization of host-guest system between inosine and β-cyclodextrin through inclusion mode. *Spectrochim. Acta, Part A* **2015**, *147*, 151−157.
(25) Zhao, R.; Sandstrom, C.; Zhang, H.; Tan, T. NMR Study on the Inclusion Complexes of β-Cyvlodextrin with Isoflavones. *Molecules* **2016**, *21*, No. 372.
(26) Uekaji, Y.; Jo, A.; Ohnishi, M.; Nakata, D.; Terao, K. Anew Generation of Nutraceuticals and Cosme-ceuticals Complexing Lipophilic bioactives with γ-Cyclodextrin. *Trans. Mater. Res. Soc. Jpn.* **2012**, *37*, 89−94.
(27) Aytac, Z.; Uyar, T. Antioxidant activity and photostability of α-tocopherol/β-cyclodextrin inclusion complex encapsulated electrospun polycaprolactone nanofibers. *Eur. Polym. J.* **2016**, *79*, 140−149.

DOI: 10.1021/acsomega.9b00733
ACS Omega 2019, 4, 8632−8640